Use of the mesentery and peritoneum to facilitate the absorption of yolk sac nutrients into viscera of the developing chick: novel function for this organ

Liyang Wang[1#], Mengmeng Xu[2#], Odell Jones[3#], Xin Zhou[1,4], Zhongguang Li[1,4], Yanping Sun[5], Yuhui Zhang[1], Joseph Bryant[6], Jianjie Ma[4], William B. Isaacs[7], Xuehong Xu[1]

[1]The Laboratory of Cell Genetics and Developmental Biology (CGDB), Shaanxi Normal University College of Life Sciences, Xi'an 710062, China; [2]Department of Pharmacology, Duke University Medical Center, Durham, NC, USA; [3]University of Pennsylvania ULAR, Philadelphia, PA, USA; [4]Ohio State University School of Medicine, Columbus, OH, USA; [5]College of Pharmacy, Xi'an Medical University, Xi'an, China; [6]Institute of Human Virology, University of Maryland School of Medicine, Baltimore, MD, USA; [7]Johns Hopkins School of Medicine, Baltimore, MD, USA

Contributions: (I) Conception and design: X Xu, L Wang, M Xu; (II) Administrative support: X Xu, L Wang, M Xu; (III) Provision of study materials or patients: None; (IV) Collection and assembly of data: X Xu, L Wang, M Xu; (V) Data analysis and interpretation: X Xu, L Wang, M Xu; (VI) Manuscript writing: All authors; (VII) Final approval of manuscript: All authors.

[#]These authors contributed equally to this work.

Correspondence to: Professor Xuehong Xu, PhD. Office 4-213/214, No. 620, West Chang'an Avenue, Chang'an District, Xi'an 710119, China. Email: xhx0708@snnu.edu.cn; xhx070862@163.com.

Background: The newly designated organ system consisting of the mesentery and peritoneum (MAP), is a thin, sheet-like membrane responsible for protecting the abdominal cavity, suspending and organizing abdominal viscera, and facilitating communication between these structures. Recognition of the mesentery as an organ has introduced a potential link between visceral obesity and systemic diseases such as cardiovascular disease and metabolic syndromes.

Methods: Polarization macroscopy, small angle X-ray scattering (SAXS), X-ray diffraction (XRD) and histological analysis were deployed to study the movement of liquid crystal lipid droplets (LCLDs) in the chick yolk sac, mesentery, and peritoneum during the seven-to-ten-day yolk sac absorption process.

Results: Nutrients in the yolk sac were visualized as liquid crystal lipid droplets and calcium carbonate vaterite crystal particles with polarized birefringence. During yolk sac absorption, these birefringent structures were distributed between the yolk sac and the yolk sac-Jejunum/Ileum (YC-JI) mesenteric complex. The latter is a mesenteric region enclosing the vitelline duct, vitelline artery, umbilical vein, and yolk sac, and extending into Jejunum/Ileum. LCLD nutrients were also distributed in the intra-mesentery-space (IMS) (i.e., the anatomical space between mesentery and enclosed viscera). Within the IMS they appeared to accumulate at a certain region, termed the mesenteric traffic center. We further found that the LCLDs were distributed throughout the mesentery in apposition with organs including the aorta and the pericardium and heart before being absorbed into their respective organs including heart, lung, and kidney.

Conclusions: The distribution of birefringent LCLDs indicates that the mesentery provides a conduit for the distribution of nutrients from the yolk sac to viscera.

Keywords: Mesentery and peritoneum (MAP); liquid crystal; LCLD transportation; YS-JI mesentery complex

Introduction

The mesentery supports intra-abdominal organs through a combination of vascular connections and peritono-fascial attachments (1-3). This newly recognized organ forms the 3-dimensional frame responsible for maintaining the organization of the numerous organs in the abdomen (4).

The mesentery comprises several regions named according to the structure with which they are contiguous. The mesentery attached to the small bowel, transverse mesocolon, and mesosigmoid connect the named portion of the gastrointestinal (GI) tract to the posterior abdominal wall, thereby permitting some movement but preventing intestinal torsion. The mesogastrium and mesoduodenum provide similar stability for contiguous regions of intestine (5). The lesser omentum serves as a linkage mechanism between the lesser curvature of the stomach to the liver. However, the great omentum, which extends from the greater curvature of the stomach and is draped over most of the intestine, likely serves multiple additional purposes. Recent studies have linked abnormal inflammation in the mesentery to a variety of medical conditions (mesenteropathies) including adhesion formation, mesenteric panniculitis, irritable bowel syndrome, and Crohn's disease (6-11). Adipose tissue deposition in the mesentery, especially the greater omentum, is linked with chronic illnesses as such as obesity, cardiovascular disease, diabetes, and metabolic syndrome (12-14).

Although focus on the mesentery as an anatomical and functional organ could shed light on molecular mechanisms underlying mesenteric pathologies, a lack of animal models continues to hinder advances in the field. Recently, we demonstrated that the yolk sac-Jejunum/Ileum (YC-JI) complex is a highly active region of mesentery enclosing the vitelline duct, vitelline artery, umbilical vein, and yolk, and is contiguous with both Jejunum/Ileum (15). The YC-JI complex facilitates yolk sac regression. Here, we present data supporting the suggestion that the mesentery plays a role in mass absorption and redistribution of yolk sac nutrients in the developing chick. The findings suggest that nutrients, in the form of liquid crystal lipid droplets (LCLDs) and carbonate vaterite crystal (CCVC) particles, are rapidly disseminated from the yolk sac, to visceral organs, via the mesentery.

Methods

Animals and sampling

Shaanxi domestic chickens were purchased from Hu County Chicken Farm of Xi'an. All chickens were bred in a chick-care facility with a natural day-night cycle. The animals were decapitated, and mesenteric fluid was collected between the mesentery and intestines as indicated in *Figure 1*. The sheet-like mesentery was surgically excised (i.e., excised intact) for examination using polarized microscopy. The heart, lungs, kidneys and YC-JI complex were harvested (15-17). All animal maintenance and experimental protocols were conducted in accordance with the guidelines of Animal Care and Use Committee of Shaanxi Normal University.

Histology analysis

Cryo-sectioning of chicken tissue was performed as previously described to prepare samples for histological analysis (15,18,19). In brief, the samples were embedded with cryomatrix embedding agent (OTC) on a flat surface immediately after dissection, then sectioned into slices of 10–15 μm thickness. Hematoxylin and eosin (H&E) staining was performed on the sections and examination of the heart, lungs, kidneys, and YC-JI mesentery complex was carried out under bright field microscopy (Carl Zeiss Microscopy GmbH).

Polarization microscopy

All experiments involving polarization microscopy were performed following previously described procedures (15-17,20). The analyses were performed on fresh tissue sections of 15 μm thickness, or in the case of mesenteric samples, flattened mesenteric tissue or mesenteric fluid smears. All tissue samples were mounted with 30% glycerol in PBS (PH 7.4) and sealed with glass coverslips. Thermal phase transition and pressure applied-release studies of mesenteric LCLDs were performed on smear-samples slides with results documented by manufacturer software ZEN (21).

Thermal phase-transition and fluidity analysis

Chick yolk sac lipid droplets have two physical states, i.e., liquid-crystal status with anisotropic birefringence and liquid status with isotropic birefringence (22). The ability to transition between these two states is a crucial characteristic of liquid crystals. Thus, to confirm the LCLDs as liquid-crystal the particles were induced to phase transition from anisotropic liquid crystal and an anisotropic droplet ($Ph_{ani\to iso}$) by increasing temperature and back from isotropic

droplets to anisotropic liquid crystal (Ph$_{iso \to ani}$) with cooling. This procedure was conducted following the previously established protocol for phase transition studies (15,16,21). In short, fluid smears were inspected between polarizer and analyzer (two prisms) and consecutive images captured for analysis throughout the temperature-induced phase change process. Recorded copies of birefringence transitions between the anisotropic and isotropic phases were obtained and analyzed with ImageJ.

Fluidity, the capacity of a material to distort and recover its shape, is another characteristic typical of liquid crystal, but not crystalline matter (22). Therefore, the fluidity of birefringent particles was confirmed using a previously described, standardized pressure-release test (15,16,21). In short, pressure was applied over the coverslip of the fluid-smear being analyzed, and changes in shape of the birefringent particles tracked using polarized microscopy. Fluidity is demonstrated by shape change (usual elongation) following pressure application and the ability to return to the original shape when pressure is removed (15,20).

Small angle X-ray scattering (SAXS) and X-ray diffraction (XRD)

To identify the features of liquid crystals and crystals in the yolk sac during chick development, we employed SAXS and XRD to characterize diffraction patterns of yolk sac samples collected as previously described (15). SAXS was documented on the small-angle goniometer of D/max-rA diffractometer at diffraction angles (2θ) of 0.3°–3° with divergence slit (DS) of 0.2°. XRD were documented on the wide-angle goniometer at a diffraction angle (2θ) of 3°–80° with DS slit of 0.6°. The two procedures were both performed with CuK α radiation (α=1.5418 Å), graphite monochromator, Scan 4.00, and power 40kV × 40mA. All data were processed with XRD analysis software MDI Jade6.

Visualization of LCLD transportation from the yolk sac into the embryo

Mesenteric tissue was collected and stretched to examine the transportation of yolk sac LCLDs and other nutrients including CCVC particles. Two procedures were used to study the movement of yolk sac fluid from the yolk sac to the mesentery. (I) The polarization feature of liquid crystals was used to visualize LCLDs in the YS-JI mesenteric complex as described above. These findings were localized to the physical structure by comparing images to anatomical structures found on H&E test (15,16,21). (II) Chicago Blue (CB) dye was injected into the yolk sac to label the yolk sac fluid and enable the tracking of fluid movement from the yolk sac into the embryo. 100 µL of Chicago Blue dye (0.1 mg/mL in PBS) was injected into the chick yolk sac on P1 to delineate detailed structures within the yolk sac and movement of yolk sac contents. Aqueous Chicago Blue dye was chosen given its compatibility with chick physiology and clear visualization of fluid motion within both the yolk sac and the embryo. Two days after dye injection, embryos were dissected and re-examined, and the location of the blue dye documented using stereomicroscopy (Motic Electric Group Co., Ltd). Polarization microscopy was again used to identify the persistence of birefringent particles within the Chicago Blue dyed yolk sac fluid.

Image analysis

Images from conventional and polarization microscopy were acquired using Inverted microscopy (Carl Zeiss Microscopy GmbH) and manufacturer software ZEN. Quantitation and analysis of birefringent intensity was conducted using image analysis software ImageJ 1.50d (NIH, Bethesda, MD).

Results

Identification of structures linking the yolk sac and developing chick mesentery

Complete development of a chicken embryo occurs 21 days after fertilization. Internal organs and limbs are differentiated within the first week. The remaining two weeks are dedicated to these organs reaching full size within the space limitation. This entire developmental process is fueled by essential nutrients stored in the yolk sac. While the yolk sac is slowly depleted throughout the gestational period, at embryonic day 19, the remaining yolk sac is enclosed in the body cavity. This process is completed before hatching on embryonic day 21 so that the absorbed yolk sac can continue providing essential nutrition to the newly hatched chick (23-26).

The yolk sac-jejunal/ileal mesenteric complex (YC-JI mesenteric complex) comprises the yolk sac, vitelline duct, jejunum, ileum and contiguous mesentery (15) (*Figures 1,2*). The YC-JI mesenteric complex can be visualised during the first two weeks of chick development (*Figure 2A*). The complex provides two significant avenues through which the yolk sac can accomplish its canonical embryonic
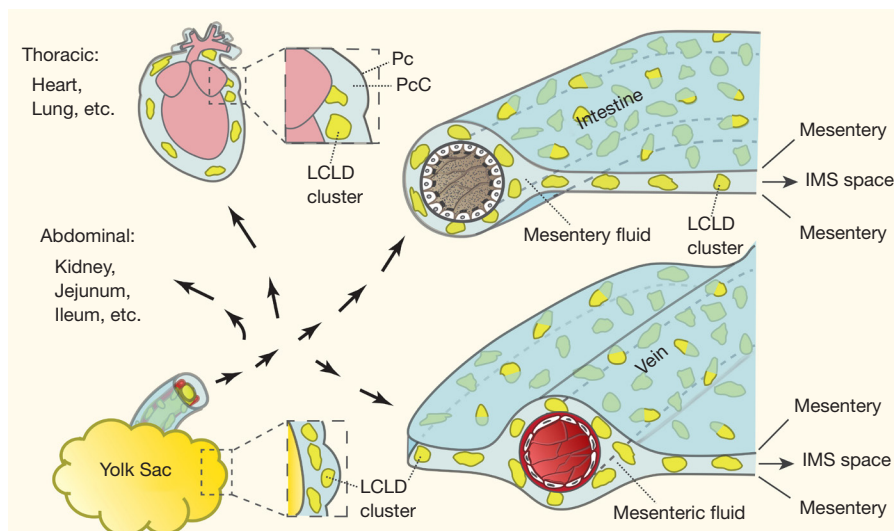
Figure 1 A model of the yolk sac-Jejunum/Ileum (YC-JI) mesentery system in chick development. LCLD transportation within the Yolk Sac-Jejunum/Ileum (YS-JI) mesentery complex and the traffic flow to target organs are illustrated. Yolk sac nutrients (arrow) were transported to the intestine (Jejunum and Ileum) initially through a structure including the mesentery, vitelline vein, vitelline arteries vein, and vitelline arteries, and umbilical vein and connecting the yolk sac and the intestine. LCLD, liquid crystal lipid droplet.

function as a nutritional reservoir (*Figure 1*). First, the YC-JI mesenteric complex provides a direct tubular connection in the vitelline duct which ranges from one-quarter to one-tenth of the external diameter (*Figure 2B,C,D*) of the outer diameter of the duodenum (*Figure 2H*). The YC-JI path mesentery complex also contains a more complex lattice of interweaving channels within the mesentery itself.

The YC-JI lattice can be divided into two sections. It begins as the central stem, composed of the vitelline vein, vitelline arteries, and umbilical vein, projecting from yolk sac into the central zone of the YC-JI complex. From there, the YC-JI connection branches and extends into Jejunum, Ileum, and other targets (*Figures 1,2*). As with vasculature, these tunnel-like structures decrease in diameter as they divide and reach their destination organs. These mesenteric vessels appear to be involved in transport of nutrients from the yolk sac to destination organs (*Figure 2E,F,G*), bypassing absorption through the GI tract. Nutrition derived from the yolk sac appears to be delivered entirely through the YC-JI mesentery complex during the early two weeks of postnatal chick development (*Figure 2K*).

YS-JI mesentery complex as an LCLD transportation system for yolk sac LCLD and CCVC

The yolk sac is a complex structure with strong birefringence under polarization microscopy. Structures in the yolk sac that generate this optical property are LCLDs and CCVCs, which are birefringent Maltese crosses and spherical particles (27,28), respectively. These consist of lipids and mineral nutrition essential to chick development. They require the YS-JI mesentery complex for LCLD transportation throughout the developing chick. Thus, LCLD transportation of yolk sac nutrition can be traced using polarized lights (*Figure 3*).

LCLDs can be observed as Maltese crosses in the yolk sac as early as two days after incubation of a fertilized egg. These initially appear in the mid zone of yolk sac and accumulate in number and size as the chicken embryo develops. They display fluidity and temperature-dependent phase transitions characteristic of liquid crystal structures. The fluidity of yolk sac Maltese crosses allows fusion between two or more crosses and division of an individual into daughter crosses. Maltese crosses, in cluster format, remain the dominant birefringent structure until post-fertilization day 12, at which time the now massive LCLDs become the dominant structure and CCVC first appear.

After first appearing at developmental day 12, CCVCs gradually become the dominant birefringent particle by day 17. Calcium carbonate crystals were harvested from many chick embryos (n>12) at incubation days 17–21. In order to characterise CCVCs from before day 19 (i.e.,
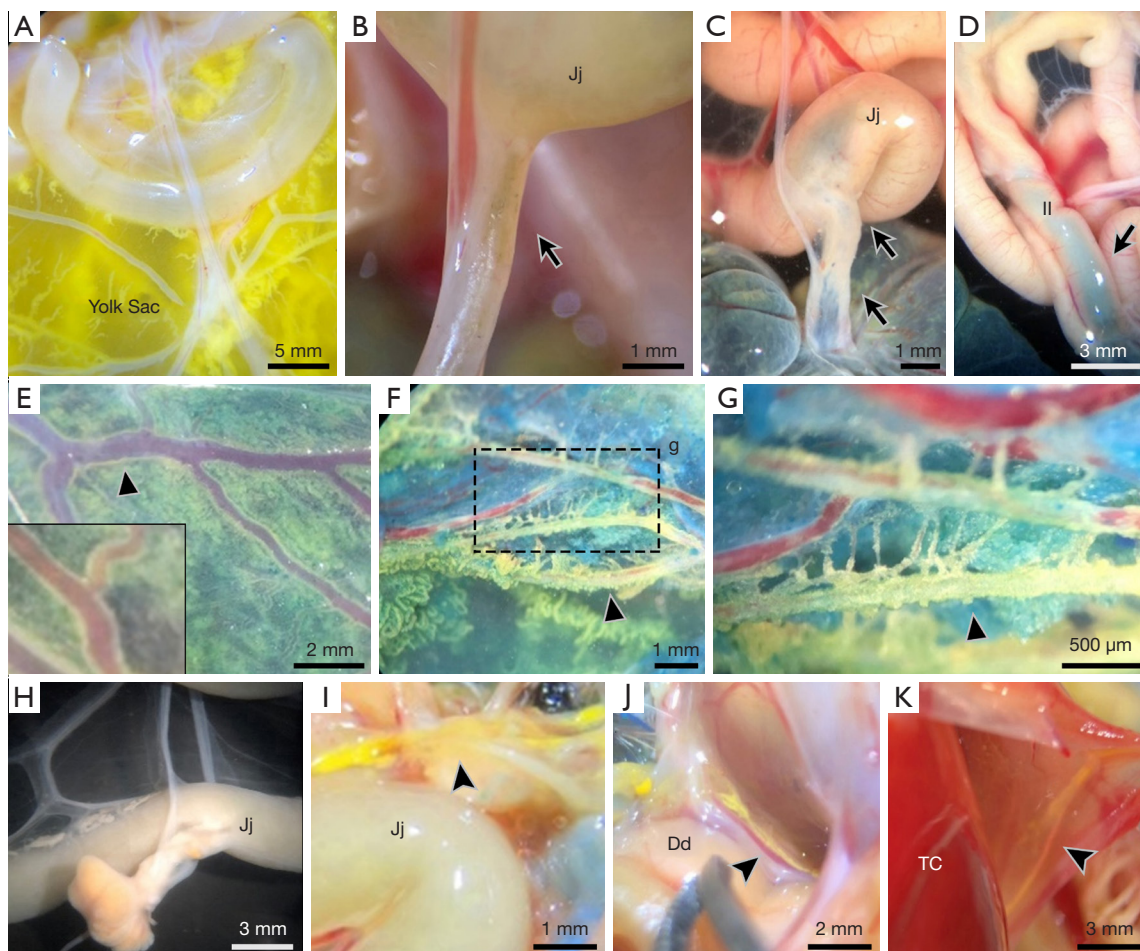
Figure 2 The movements of yolk sac contents during embryonic development within the shell and in newly emerged chicks. Chicago Blue (CB) was injected directly into the yolk sac for tracing of nutrient movement from the yolk sac into the viscera. Panels A-G show the yolk sac associated mesentery system during days 19–22 (E19-22) of chicken embryo development. Panels H-K show the mesentery of chicks nine days post (P9) emergence from the shell. Among these, panels C and D demonstrate Yolk sac nutrition (arrow) transportation to the intestine (Jejunum and Ileum) by CB staining. Vessels containing liquid crystal droplets are visualized in panel E with closely associated blood vessels (triangle). Vessels that branch and also contain liquid crystals are seen in close association with blood vessels and are demonstrated in panels F and G. Panel F is enlarged in panel G to illustrate the smaller branch vessels. The vestigial yolk sac at day nine after hatching is shown in panel H. Yolk sac contents were observed in the mesentery and peritoneum of viscera (panels I-K). Scale bars in panel A is 5 mm; panels D, H, K are 3 mm; panels E, F, and J are 2 mm; panels B, C, and I are 1 mm; panel G is 500 µm. Jj, Jejunum; Il, Ileum; Dd, Duodenum; and TC, Thoracic Cavity. Jj, Jejunum; Il, Ileum; Dd, Duodenum; TC, thoracic cavity.

when the yolk sac is absorbed) PBS was used to harvest all crystals from yolk sac fluid. CCVCs harvested after day 19 were collected directly from the embryo. Clean calcium carbonate crystals were inspected using XRD 2θ detection spectrum of 3° to 80°. They formed identifiable diffractions at lattice planes d(Å) of 3.55, 3.27, 3.02, 2.72, 2.06, 1.85, 1.82, and 1.64 corresponding to I/I_0 [61], I/I_0 [100], I/I_0 [36], I/I_0 [85], I/I_0 [52], I/I_0 [21], I/I_0 [43], and I/I_0 [15] by Bragg's equation, which classified the vaterite crytal of yolk sac originated calcium carbonate. XRD patterns identified the composition of CCVCs as vaterite and not the calcite or aragonite forms of calcium carbonate
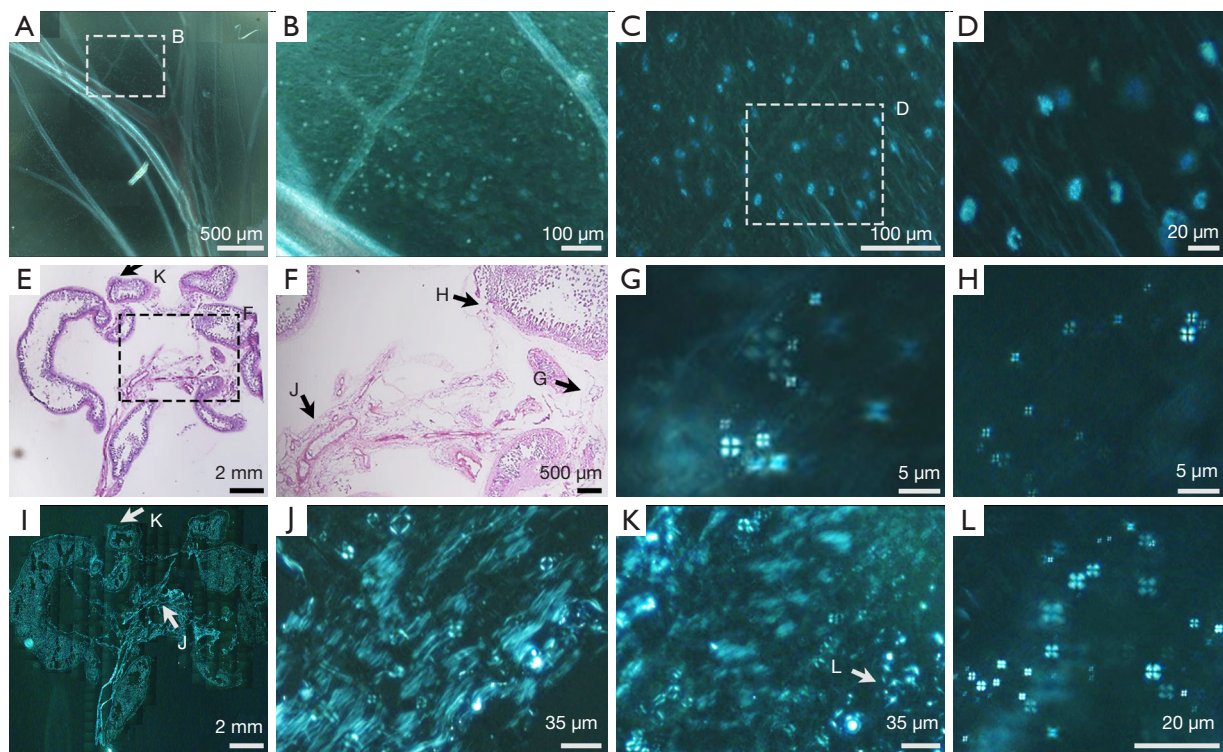
Figure 3 Visualization of the chicken embryo YS-JI mesentery complex using H&E and birefringence under polarization microscopy. Panel (A) exhibits birefringence of the intact mesentery, with a magnified view in panel (B). Further magnification of the mesentery between large vessels in panel (C) shows birefringent particles distributed throughout the mesentery. Panel (D) is a magnified view of birefringent particles found in panel (C). Panels (E), and (I) explain the corresponding location of the YS/JI mesentery complex under polarization microscopy compared to the histological position using H&E histology. Panel (F) is the in-box magnification from panel (E). K in panel (E) indicates the location of panel (K); G, H and J in panel (F) indicate the location of panel (G), (H) and (J); J and K in panel (I) indicate the location panels (J) and (K); L in panel (K) indicates the location panel (L). Panels (G), (H), (J), and (K) are enlarged birefringent images of respective areas of panels (F), and (I) indicated with arrows. Panel (L) contains further magnifications of panel (K) indicated with an arrow. Scale bars in groups (E) and (I) are 2 mm; panels (A) and (F) are 500 µm; panels (B) and (C) are 100 µm; panels (J) and (K) are 35 µm; panels (D) and (L) are 20 µm; panels (G) and (H) are 5 µm.

(*Figure 4* and *Table 1*).

LCLD transportation within the YC-JI mesentery complex during early postnatal development

In early postnatal development (2–3 weeks after hatching), the yolk sac undergoes a process during which all its components, including LC droplets and CCVC particles, are no longer observable as a mature mesentery complex forms. During this developmental stage, the embryonic YC-JI mesentery appears to be a structure that facilitates distribution of yolk sac nutrient, including mass delivery of the remaining yolk sac nutrition into mature organs. This substantial activity was tracked by injecting 0.1 mg/mL CB dye directly into the yolk sac cavity. Two days after injection, CB could be located throughout the intestine, especially in the jejunum and Ileum. While the Chicago blue dye is hydrophilic and would not track the movement of liquid crystals directly, this dye did not disrupt the delicate embryo and enabled visualization of the network carrying yolk-sac fluid (29-31). We then confirmed the existence of LCLDs in these networks using polarization microscopy. Additionally, physical channels are likely to transport both fat- and water-soluble components. However, dilution of CB could give the impression of an apparent absence of LC droplets in the intra-mesenteric
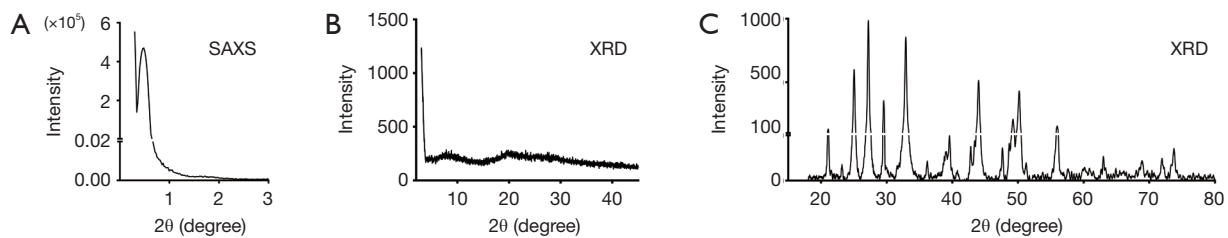
Figure 4 Small angle X-ray scattering (SAXS) and X-ray diffraction (XRD) characterization of yolk sac isolated crystals and liquid crystal lipid droplets. The diffraction pattern of yolk sac liquid crystal shows single diffraction peak by SAXS within angles (2θ) range of 0.3°–3° (A) and XRD diffraction within edges (2θ) range of 3–45° (B). The yolk sac liquid crystal lipid droplets characterize as small angle strong scattering plus large angle no diffraction. The XRD pattern of the embryonic yolk sac crystals shows a patterned set of diffraction peaks within the XRD diffraction angle (2θ) range of 3–80° (C). This crystal is characterized as the typical XRD pattern of calcium carbonate vaterite crystals (CCVC) corresponding to CCVC standard (see *Table 1*).

space and in associated organs. To investigate this, we prepared frozen sections of the YC-JI mesenteric complex, and other organs, for further examination. Our investigation found that liquid crystals were apparent as far as the heart, lung, and kidney, etc. (*Figure 5*). In the heart, LC droplets were distributed in the pericardial cavity from the apex to the level of the mid-ventricle, as well as around the aorta (*Figure 5A,B,C,D,E,F,G,H,I*).

The mesentery complex engages in local LCLD transportation as indicated by the postnatal distribution of yolk sac liquid crystals

The yolk sac is the first organ in which liquid crystal (LC) droplets appear during chicken embryonic development (21). LC-droplets are observed in the center of yolk sac as early as day 2 after fertilization (16,21). From there, liquid crystals are then found in more than 18 tissues and organs, appearing in each newly formed organ during the 21-day developmental process (16,21). However, by the end of the 21 days, LC droplets can only be detected in the internalized yolk sac of newly hatched chicks. The yolk sac remains the sole organ in which large LC droplets are found during the subsequent yolk sac absorption process. These liquid crystals can stay for up to 10 days with a few droplets retained in the resultant vestigial organ (21). The persistence of liquid crystals concurs with previous findings that LC droplets are needed for the LCLD transportation via the YC-JI mesentery complex, which remains active until the yolk sac is absorbed by newborn postnatal chick (21).

Initial LCLD transportation of yolk sac liquid crystals follow the main paths provided by the YC-

JI mesentery complex (15). However, at embryonic day 19, LC droplets can be observed evenly distributed in mesenteric fluid between mesothelial surface boundaries of the IMS space and within which they form groups at a density of 80–100 groups/mL. LC droplets are evenly distributed throughout the substance of the IMS and surrounding mesenteric arteries as islands of condensed birefringence (*Figure 3A,B,C,D*). Mesenteric LC droplets in the IMS behave as classic liquid crystals with a natural birefringent phase transition (*Figure 6A,B,C,D,E,F,G,H,I,J,K,L,M,N,O*) and fluidity (*Figure 6P,Q,R,S,T,U,V,W*). It is likely these mechanical properties are important in the intra-mesenteric space in which malleability is required for transport.

Discussion

LCLDs and CCVCs are the main contents of materials generated in the yolk sac reservoir. They include LC-LDs apparent from early development approximately around days D2-4 (27,28). Phase transition transition from liquid-crystal to a crystal state could represent a novel mechanism of bio-mineralization in the yolk sac. Inside-out and outside-in models based on laminar structure support a layer by layer crystallization of calcium carbonate from the shell. This occurs with inspiration during embryonic development (22,26). It is feasible their storage, in conjunction with fluid characteristics, enables their transport, without damage, to the YS-JI mesenteric complex. The birefringent nature of LCLDs and CCVCs has enabled observation of how yolk sac nutrients are transported through the YC-JI mesentery complex. While this may provide insights into transport

Table 1 X-ray diffraction pattern of liquid crystal and crystal isolates from chick yolk sac

Sample/peak data	Vaterite $CaCO_3$		Yolk sac crystal		Yolk sac liquid crystal	
	d(Å)	I/I_0	d(Å)	I/I_0	d(Å)	I/I_0
Diff 1	4.245	10.9	4.2099	12.9	182.6969	100
Diff 2	–	–	3.8294	2.8	–	–
Diff 3	3.5767	68.1	3.5548	60.9	–	–
Diff 4	3.2961	100	3.2741	100	–	–
Diff 5	–	–	3.021	35.5	–	–
Diff 6	2.7352	80.5	2.719	84.8	–	–
Diff 7	–	–	2.4805	4	–	–
Diff 8	2.2193	1.9	2.2754	9.8	–	–
Diff 9	2.1225	4.1	2.1109	7.6	–	–
Diff 10	–	–	2.0826	8.4	–	–
Diff 11	2.065	40.2	2.0559	51.7	–	–
Diff 12	–	–	1.9078	7	–	–
Diff 13	1.8569	12.8	1.8694	8	–	–
Diff 14	–	–	1.849	21.1	–	–
Diff 15	1.8253	28.1	1.8166	42.6	–	–
Diff 16	1.7883	2.5	1.7807	2.6	–	–
Diff 17	1.7499	0.5	–	–	–	–
Diff 18	1.6481	10.5	1.6418	14.9	–	–
Diff 19	1.5339	0.1	–	–	–	–
Diff 20	1.5118	0.7	–	–	–	–
Diff 21	1.4801	1.5	1.474	5.1	–	–
Diff 22	1.415	0.1	1.4354	2	–	–
Diff 23	1.3676	2.1	1.3618	3.5	–	–
Diff 24	1.3519	0.8	–	–	–	–
Diff 25	1.335	0.5	–	–	–	–
Diff 26	1.3158	1.5	1.3115	4.6	–	–
Diff 27	1.2881	3.2	1.283	6.5	–	–
Diff 28	1.2314	0.1	–	–	–	–
Diff 29	1.2198	0.1	–	–	–	–
Diff 30	1.1922	0.4	–	–	–	–
Diff 31	1.1806	0.1	–	–	–	–
Diff 32	1.1673	0.3	–	–	–	–
Diff 33	1.1478	0.6	–	–	–	–
Diff 34	1.1478	0.6	–	–	–	–
Diff 35	1.1402	1	–	–	–	–
Diff 36	1.1097	0.5	–	–	–	–
Diff 37	1.0987	0.1	–	–	–	–

Notes: According to the Bragg's law, d(Å) means the d-spacings of crystal lattices in inspected matters; I/I_0, the intensity ratio of each peak. Diff is short for diffraction.
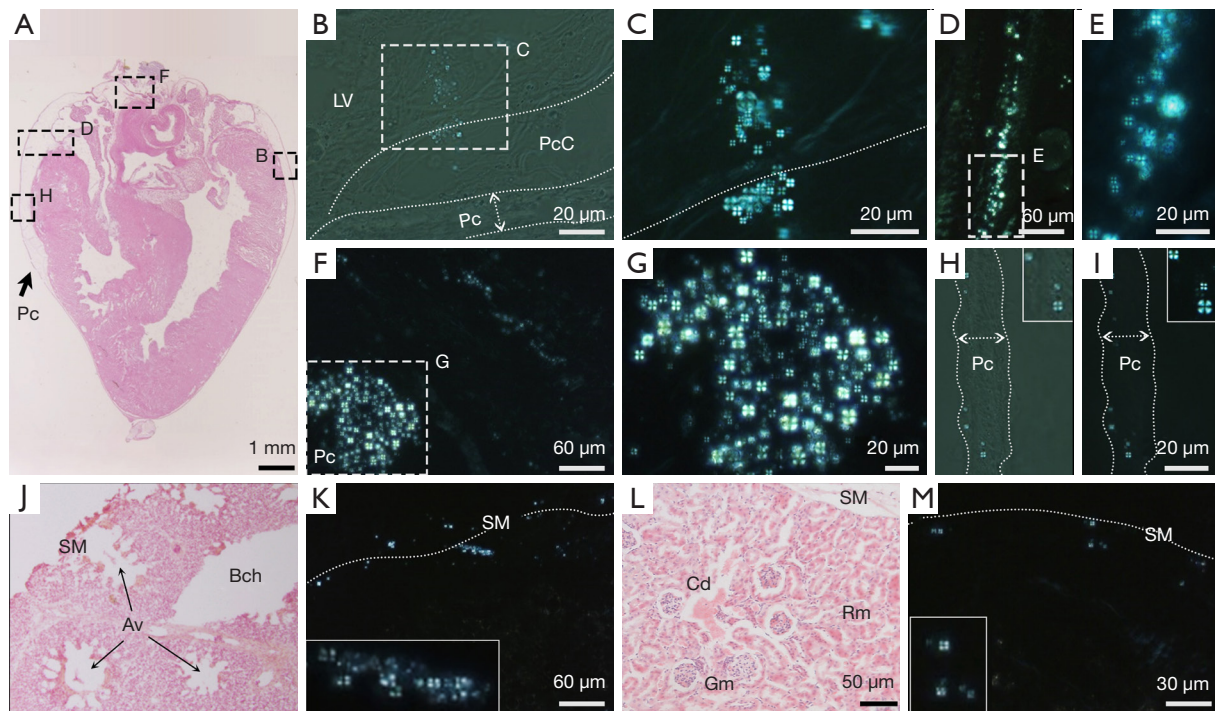
Figure 5 Birefringent yolk sac LCLDs are found in the pericardium (Pc), pericardial cavity (PcC) and serous membrane (SM) in distal organs. Histological images from chick heart are shown in panel (A), presented as a morphological location indicator. Panel (B) contains a picture of the pericardium and cavity under 45° crossed prisms (polarizer and analyzer). Corresponding polarization (90° crossed lenses) microscopy image of cavitas pericardialis is shown in panel (C) enlarged from B. Panels (D) and (E) shows liquid crystals consolidating in the cavity space between the pericardium and heart. Liquid crystals are also found around the aorta (panel F) and in the pericardium within panels (H) (45° crossed prisms) and (I) (polarized). Panels (J) and (K) contain histological and polarized (90° crossed prisms) images of the chick lung individually. Panels (L) and (M) comprise histological and polarized (90° crossed prisms) copies of the chick kidney respectively. Liquid crystals can be found in the serous membrane (SM) surrounding each organ. The insets in all images with a solid white line are framed the enlarged birefringent zone, and the white broken lines are marked as indicated. Scale bar in Panel (A) is 1 mm; panels (J) and (L) are 100 µm; panels (D), (F), and (K) are 60 µm; panel (M) is 30 µm; panels (B), (C), (E), and (G-I) are 20 µm. Pc, pericardium; LF, left ventricle; PcC, pericardial cavity; Av, alveoli; Bch, bronchiole; Cd, collecting duct; Gm, glomerulus; Rm, renal medulla; Bch, bronchiole; LV, left ventricle.

within the mesentery organ, this finding has also generated new questions.

The origin of the calcium carbonate (intra-yolk sac versus calcium carbonate from the shell) prior to crystallization remains unexplained. Additionally, the tendency for calcium carbonate to crystallize as vaterite over aragonite or calcite particles is also unexplained. Our observations were derived from the combination of hydrophilic dye and polarization microscopy. They may point to a significant shift in our understanding of how nutrients are transported. Future studies using direct visualization of LCLDs and CCVCs could enable the direct tracking of these particles. An amphiphilic dye would be needed for this process. Such a stain would allow for continued formation and tracking of droplets composed of amphiphilic molecules with externally oriented hydrophilic heads and hydrophobic cores (29-31).

Conclusions

In avian embryonic development, the mesentery appears to be associated with LCLD transportation of nutrients from the yolk sac to developing viscera. The identification of birefringent particles in the intramesenteric space, and viscera (but not in connective tissue) indicates that intestinal absorption and vascular transport are bypassed as means of transport. The findings suggest that LCLDs (including
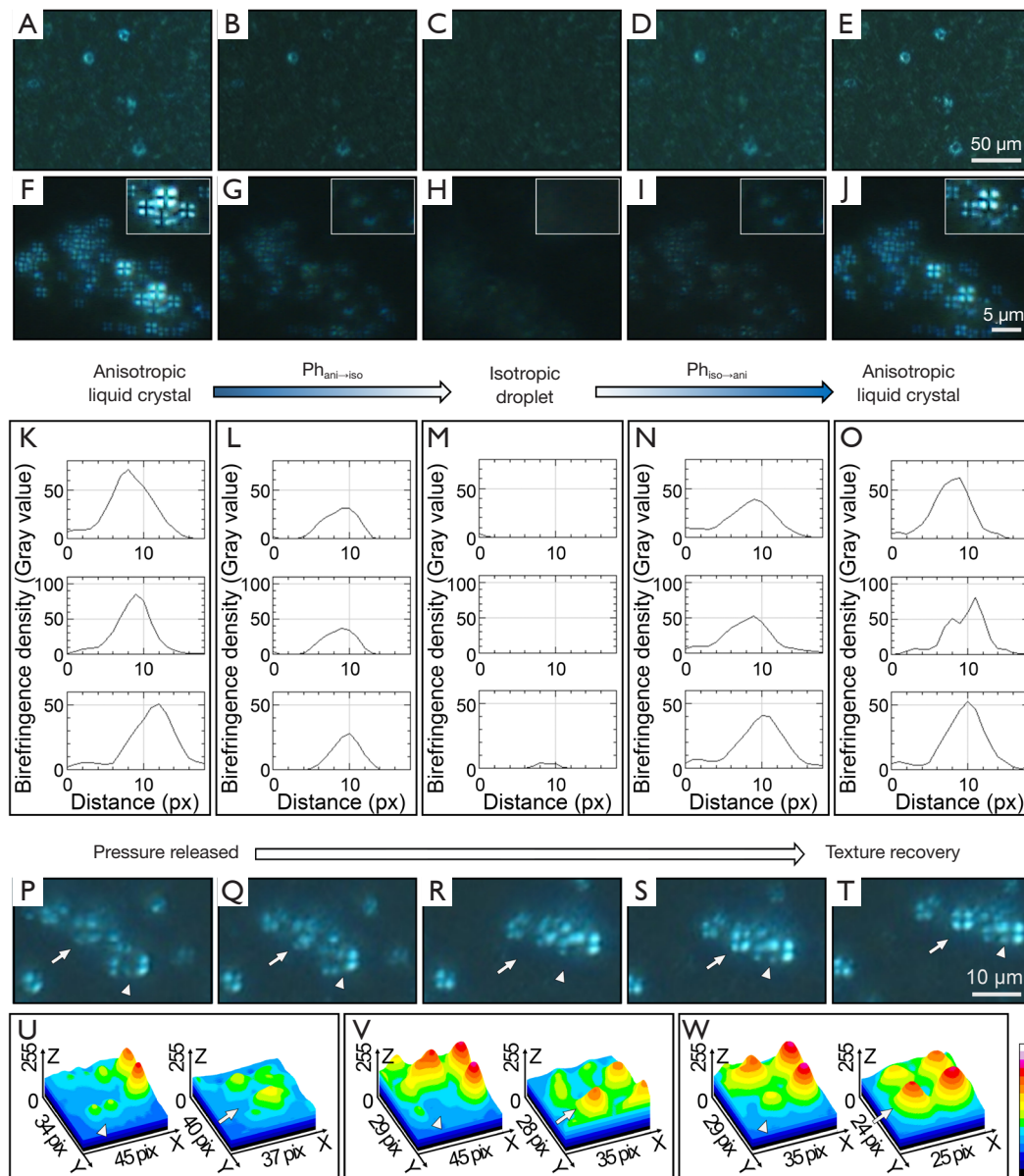
Figure 6 Phase transitions and fluidity characteristics of the LC integrated group (LC-IG) in the YS-JI mesentery system under polarized microscopy. The material status change between two phases including Phase transition between anisotropic liquid crystal and anisotropic droplet (Ph$_{ani \to iso}$; panels A,B,C and F,G,H), and transition of isotropic droplets back to anisotropic liquid crystal (Ph$_{iso \to ani}$; panels C,D,E and H,I,J). Panels A,B,E,D,E and F,G,H,I,J depict the process of phase transition. Birefringence is demonstrated in panels K-O (panels K,L,M,N,O). Fluidity is a property of liquid and liquid crystal phase matter but not crystalline matter. The fluidity of liquid crystal particles can be tracked by using polarized microscopy to monitor the changing shape of birefringent liquid crystal particles under pressure. Fluidity is demonstrated by shape change (usual elongation) following pressure application and the ability to return to the original form when force is removed. Panels P,Q,R,S,T depict the transition of elliptical structures (white arrows) generated by external force back to Maltese Crosses. 3-D graphs in panels U,V,W relate to texture recovery of two representative LC droplets. Scale bars in panels A,B,C,D,E are 50 µm; panels O,P,Q,R,S are 10 µm; panels F,G,H,I,J are 5 µm.

associated nutrients) may be transported via the mesentery. Although mesenteric based transport appears completed at two weeks after hatching, it is feasible it remains latent thereafter.

In the mammal embryo, the yolk sac is one of three embryonic cavities (chorion, amnion and yolk sac). A transient primary yolk sac composed of a double-layered extraembryonic membrane with internal hypoblast-derived endoderm and mesoderm on its external portion appears at day 5.5 in the mouse and day 8 in humans. As occurs in the avian setting, the mammalian yolk sac cavity also conveys nutrients to the developing embryo (28,30,32-34). Given parallels between avian and mammalian embryological development, it is possible that nutrient transport via liquid crystals may also occur in the mammalian setting. Moreover, it is also possible that such transport occurs via LCLDs and via the mesenteric platform. Further studies are required to investigate this possibility.

Acknowledgements

Footnote

Conflicts of Interest: The authors have no conflicts of interest to declare.

Ethical Statement: All applicable international, national, and/or institutional guidelines for the care and use of animals were followed.

References

1. Coffey JC, O'Leary DP. The mesentery: structure, function, and role in disease. Lancet Gastroenterol Hepatol 2016;1:238-47.
2. Coffey JC, Culligan K, Walsh LG, et al. An appraisal of the computed axial tomographic appearance of the human mesentery based on mesenteric contiguity from the duodenojejunal flexure to the mesorectal level. Eur Radiol 2016;26:714-21.
3. Coffey JC, O'Leary DP. Defining the mesentery as an organ and what this means for understanding its roles in digestive disorders. Expert Rev Gastroenterol Hepatol 2017;11:703-5.
4. Coffey JC, Dockery P. Colorectal cancer: Surgery for colorectal cancer - standardization required. Nat Rev Gastroenterol Hepatol 2016;13:256-7.
5. Coffey JC, O'Leary DP, Kiernan MG, et al. The mesentery in Crohn's disease: friend or foe? Curr Opin Gastroenterol 2016;32:267-73.
6. Heald RJ, Ryall RD. Recurrence and survival after total mesorectal excision for rectal cancer. Lancet 1986;1:1479-82.
7. D'Alessio S, Correale C, Tacconi C, et al. VEGF-C-dependent stimulation of lymphatic function ameliorates experimental inflammatory bowel disease. J Clin Invest 2014;124:3863-78.
8. Li Y, Zhu W, Zuo L, et al. The Role of the Mesentery in Crohn's Disease: The Contributions of Nerves, Vessels, Lymphatics, and Fat to the Pathogenesis and Disease Course. Inflamm Bowel Dis 2016;22:1483-95.
9. Li Y, Zhu W, Gong J, et al. Visceral fat area is associated with a high risk for early postoperative recurrence in Crohn's disease. Colorectal Dis 2015;17:225-34.
10. Culligan K, Walsh S, Dunne C, et al. The mesocolon: a histological and electron microscopic characterization of the mesenteric attachment of the colon prior to and after surgical mobilization. Ann Surg 2014;260:1048-56.
11. Zuo L, Li Y, Zhu W, et al. Mesenteric Adipocyte Dysfunction in Crohn's Disease is Associated with Hypoxia. Inflamm Bowel Dis 2016;22:114-26.
12. Tracy RP. Is visceral adiposity the "enemy within"? Arterioscler Thromb Vasc Biol 2001;21:881-3.
13. Loskutoff DJ, Samad F. The adipocyte and hemostatic balance in obesity: studies of PAI-1. Arterioscler Thromb Vasc Biol 1998;18:1-6.
14. Bonen A, Tandon NN, Glatz JF, et al. The fatty acid transporter FAT/CD36 is upregulated in subcutaneous and visceral adipose tissues in human obesity and type 2 diabetes. Int J Obes (Lond) 2006;30:877-83.
15. Ling G, Wang LY, Rui F, et al. Transportation of liquid crystal and CaCO3 vaterite crystal in chicken embryo and early postnatal development. Molecular Crystals and Liquid Crystals 2017;647:373-84.
16. Xu XH, Xu MM, Jones OD, et al. Liquid Crystal in Lung Development and Chicken Embryogenesis. Molecular Crystals and Liquid Crystals 2011;547:164-72.

17. Xu MM, Xu XH, Cao GL, et al. The Liquid Crystalline in Normal Renal Development Amplifies the Comprehension for Anderson-Fabry Disease. Molecular Crystals and Liquid Crystals 2009;508:52-66.

18. Xu X, Dong C, Vogel BE. Hemicentins assemble on diverse epithelia in the mouse. J Histochem Cytochem. 2007; 55:119-26.

19. Maruyama M, Li BY, Chen H, et al. FKBP12 is a critical regulator of the heart rhythm and the cardiac voltage-gated sodium current in mice. Circ Res 2011;108:1042-52.

20. Xu M, Jones OD, Wang L, et al. Characterization of tubular liquid crystal structure in embryonic stem cell derived embryoid bodies. Cell Biosci 2017;7:3-12.

21. Xu MM, Xu XH. Liquid-Crystal in Embryogenesis and Pathogenesis of Human Diseases. In: Sato KS. editor. Embryogenesis. InTech, Rijeka, 2012; 637-52.

22. Brown GH and Wolken JJ. Liquid crystal and Biological Structures. London: Academic Press, 1979.

23. Hamburger V, Hamilton HL. A series of normal stages in the development of the chick embryo. J Morphol 1951;88:49-92.

24. Hamburger V, Hamilton HL. A series of normal stages in the development of the chick embryo. 1951. Dev Dyn 1992;195:231-72.

25. Sanes JR. On the republication of the Hamburger-Hamilton stage series. Dev Dyn 1992;195:229-30.

26. Hamburger V. The stage series of the chick embryo. Dev Dyn 1992;195:273-5.

27. Li M, Cao L. A study of egg yolk sac spherocrystal in period of the embryo developing of lai-hang chicken. Acta Biophysica Sinica 1986;2:381-9.

28. Xu XH, Xu MM, Cao GL, et al. Co-Subsistence of liquid crystal droplets and calcium carbonate vaterite crystals reveals a molecular mechanism of calcium preservation in embryogenesis. Molecular Crystals and Liquid Crystals 2009;508:77-90.

29. Goldstein JL, Brown MS. From fatty streak to fatty liver: 33 years of joint publications in the JCI. J Clin Invest 2008;118:1220-2.

30. Small DM. George Lyman Duff memorial lecture. Progression and regression of atherosclerotic lesions. Insights from lipid physical biochemistry. Arteriosclerosis 1988;8:103-29.

31. Small DM. The Physico-Chemical Properties of Lipids during the Development and Regression of Atherosclerosis. J Japan Arteriosclerosis Society 1990;18:579-97.

32. Xu MM, Jones O, Cao G, et al. Crystallization of calcium carbonate vaterite involves with another mechanism associated with liquid crystal in embryonic yolk sacs. Key Engineering Materials 2010;428-429:349-55.

33. Xu MM, Jones OD, Zheng SE, et al. Cytoplasmic accumulation of liquid-crystal like droplets in post-infection sputum generated by Gram-positive bacteria. Molecular Crystals and Liquid Crystals 2011;547:173-80.

34. Zohn IE, Sarkar AA. The visceral yolk sac endoderm provides for absorption of nutrients to the embryo during neurulation. Birth Defects Res A Clin Mol Teratol 2010;88:593-600.